Lead silicate glasses: Binary network-former glasses with large amounts of free volume

S. Kohara, H. Ohno, and M. Takata
Japan Synchrotron Radiation Research Institute/SPring-8, 1-1-1 Kouto, Sayo-cho, Sayo-gun, Hyogo 679-5198, Japan

T. Usuki and H. Morita
Graduate School of Science and Engineering, Yamagata University, 1-4-12 Kojirakawa, Yamagata 990-8560, Japan

K. Suzuya
J-PARC Center, Japan Atomic Energy Agency, Tokai-mura, Naka-gun, Ibaraki 319-1195, Japan

J. Akola
Department of Physics, Tampere University of Technology, P.O. Box 692, FI-33101 Tampere, Finland
and Nanoscience Center, Department of Physics, University of Jyväskylä, P.O. Box 35, FI-40014 Jyväskylä, Finland

L. Pusztai
Research Institute for Solid State Physics and Optics, P.O. Box 49, H-1525 Budapest, Hungary
(Received 19 August 2010; published 29 October 2010)

It is well known that PbO-SiO_2 exhibits a wide glass formation composition range, up to 90 mol % PbO. Earlier studies suggest that the existence of PbO_3 or PbO_4 structural units, which act like network formers, may be the reason for the wide glass formation range but the structure beyond short-range order is still unclear. Here we found that the network formation in the glass is governed by the interplay of SiO_4 tetrahedra and PbO_x polyhedra (x=3–5, x=4 is major) as a network former while the distribution of other (non-network) units is inhomogeneous. The inhomogeneous distribution of PbO_x polyhedra in the 34 mol % PbO glass and that of SiO_4 tetrahedra in the 65 mol % PbO glass yield a prepeak at $Q<1.5$ Å^{-1}, a sign of a characteristic length of the inhomogeneity in the diffraction patterns. Furthermore, PbO-SiO_2 glasses contain extraordinarily large amounts of free volume (voids), which cannot be found in conventional binary silicate glasses (network former—network modifier) but only in network-former glasses such as SiO_2 glass and in its mixtures with another network former such as GeO_2. We classify PbO-SiO_2 glass as a "binary network-former glass" with large amounts of free volume.

DOI: 10.1103/PhysRevB.82.134209 PACS number(s): 61.43.Fs, 61.05.C−, 61.05.F−

I. INTRODUCTION

The basic idea of glass formation, the continuous random network (CRN) model, was proposed by Zachariasen[1] who defined B_2O_3, As_2O_3, SiO_2, GeO_2, and P_2O_5 as glass formers, which form continuous three-dimensional network structures of corner-sharing oxygen polyhedra (i.e., triangle: BO_3 and AsO_3, tetrahedron: SiO_4, GeO_4, and PO_4), resulting in large amount of free volume. An additional nonglass former, e.g., CaO or Na_2O, modifies the CRN by forming nonbridging oxygen atoms and rearranging the framework as the modifier cations are situated interstitially into the rearranged random network, surrounded by the nonbridging oxygen.[2] Thus, a composition limit of glass formation in oxides appears due to the limit imposed by the insufficient amount of network formers. Details of the modified network structure beyond the polyhedral units and short-range ordering of the modifier cation are still unclear and controversial.[3–5]

The PbO-SiO_2 system is a very popular glass in our daily life as "crystal glass" and it has numerous industrial applications, e.g., as optical glasses,[6] in optoelectronics,[7] or in radiation shielding. This system forms glasses over a wide composition range, up to 90 mol % PbO, and the glasses can be easily prepared by using the conventional melt-quench technique. The structure of PbO-SiO_2 glasses has been widely studied by diffraction measurements,[8–12] spectroscopic measurements,[12–17] and molecular-dynamics simulations.[18] However, it must be stressed that the modified CRN model mentioned above cannot interpret the wide glass formation range. It is also well known that PbO is classified to network modifiers and to intermediates between network formers and network modifiers.[19] Previous studies suggest that PbO_3 and/or PbO_4 structural units act as network formers in high PbO glass.[8–10,18] However, substantial structural questions still remain to understand the wide glass forming range because a three-dimensional model for the structure is missing: (i) how is the structure governed by SiO_4 tetrahedra and PbO_3 and/or PbO_4 polyhedra? (ii) What is the substantial structural role of PbO as an intermediate? In an attempt to shed light onto these questions and explain the glass forming ability of PbO-SiO_2 glasses, we reveal details of the glass structure by the use of a combination of x-ray and neutron-diffraction measurements, with the aid of a structure modeling technique.

II. EXPERIMENTAL

A series of six PbO-SiO_2 glasses, with compositions between 30 and 65 mol % of PbO, were prepared from reagent grade PbO, $Pb(NO_3)_2$, and SiO_2 powders. The mixed powders (60–70 cm^3) were melted in silica crucibles in air and

kept at 1000–1400 °C for about 30 min as rough melts. The melts were then mounted on platinum crucibles and were stirred for homogenizing at 1000–1500 °C for about 90 min. Molten samples were poured into graphite casks, kept about at the glass transition temperatures for an hour and then cooled at a cooling rate of 20 °C/h to room temperature. PbO content, determined by atomic emission spectrometry using inductively coupled plasma, for the six PbO-SiO_2 glasses were 29.58, 33.78, 37.86, 50.36, and 65.12 mol % (hereafter simply denoted by 30, 34, 38, 50, and 65 mol % PbO), respectively. Densities, as measured by Archimedian method, were 4.28 g/cm^3, 4.66 g/cm^3, 4.94 g/cm^3, 5.98 g/cm^3, and 6.91 g/cm^3, respectively.

The high-energy x-ray diffraction experiments were carried out at the SPring-8 high-energy x-ray diffraction beamline BL04B2 (Ref. 20) using a two-axis diffractometer dedicated to glass, liquid, and amorphous materials. To obtain total structure factors $S(Q)$, the diffraction patterns of powder sample in a thin-walled (10 μm) silica glass tube of 2 mm diameter (supplier: GLAS Müller, D-13503 Berlin, Germany) were measured in transmission geometry. The incident energy of x rays was 113.3 keV. The intensity of incident x rays was monitored by an ionization chamber filled with Ar gas while scattered x-ray intensities were detected by a Ge detector. A vacuum chamber was used to suppress air scattering around the sample. Raw data were corrected for background scattering, including scattering from the sample tube, polarization, absorption, and incoherent scattering using a standard software.[21] Absorption coefficients, incoherent scattering functions, and atomic scattering factors were taken from Refs. 22–24, respectively. To obtain reliable diffraction patterns over the small angle region, the diffraction pattern of a broken piece of thick flat plate glass (1 mm thickness) was measured in transmission geometry (without a sample tube) using an incident x-ray energy of 61.6 keV.

The neutron-diffraction measurement was performed on the glass, liquid and amorphous diffractometer[25] at the Intense Pulsed Neutron Source (IPNS), Argonne National Laboratory. The powdered amorphous sample was encapsulated in a thin-walled (0.1 mm) vanadium can with an inner diameter of 9.8 mm. Data were corrected for container scattering, attenuation, multiple scattering, and inelastic scattering and the corrected data were normalized to the scattering from a vanadium rod. This was performed using the ATLAS software package for time-of-flight neutron-diffraction data.[26]

The fully corrected x-ray and neutron data were normalized to give the Faber-Ziman[27] total structure factors $S(Q)$. The total correlation function $T(r)$ was derived by Fourier transforming $S(Q)$ as

$$T(r) = 4\pi\rho r \cdot g(r),$$

where

$$g(r) = 1 + \frac{1}{2\pi^2\rho r}\int_{Q_{\min}}^{Q_{\max}} Q[S(Q)-1]\sin(Qr)\cdot M(Q)dQ, \quad (1)$$

where ρ is the atomic number density (density in units of "number of atoms per cubic angstrom") of the sample and $M(Q)$ is the (Lorch type[28]) modification function. $Q_{\max}$ was 20 $Å^{-1}$ for both x-ray and neutron data.

III. REVERSE MONTE CARLO SIMULATION

Reverse Monte Carlo (RMC) simulations were performed on ensembles of 5000 particles using the RMCA code.[29] The initial configurations were random configurations and hard sphere MC (HSMC) simulations were applied to avoid physically unrealistic structure. The constraints were of two kinds: closest atom-atom approach and connectivity. The choices of the closest atom-atom approaches were determined to avoid unreasonable spikes in the partial pair correlation functions. The constraints on the Si-O connectivity were that all silicon atoms had to be coordinated by four oxygen atoms whereas no constraint on the Pb-O connectivity was applied. After the HSMC simulations, RMC simulations with both x-ray and neutron $S(Q)$ were performed. Atomic number densities for 34, 50, and 65 mol % PbO glasses were 0.0649, 0.0626, and 0.0588 $Å^{-3}$, respectively.

The cavity analysis was performed as described in Ref. 30. The system was divided into a cubic mesh with a grid spacing of 0.20 Å, and the points farther from any atom than a given cutoff (here 2.5 Å) were selected (cavity domains). Each domain was characterized by the point where the distance to all atoms is a maximum. If there are no maxima closer than the divacancy cutoff (here 2.0 Å), we located the center of the largest sphere that can be placed inside the cavity. This point can be used for calculating partial pair distribution functions, including vacancy-vacancy correlations. Around the cavity domains, we constructed cells analogous to the Voronoi polyhedra in amorphous phases (cf. the Wigner-Seitz cell) and analyzed their volume distribution.

IV. RESULTS AND DISCUSSION

Figures 1(a) and 1(b) show the x-ray and neutron structure factors, respectively, of PbO-SiO_2 glasses. As can be seen in the figures, the contrast between x-ray and neutron data is excellent, which is important for deriving detailed structural information in a complicated oxide glass. The x-ray structure factors, $S(Q)$, that are most sensitive to Pb-Pb correlations, do not exhibit significant differences for $Q > 1.5$ $Å^{-1}$. The neutron $S(Q)$ of all compositions have a sharp peak at approximately $Q=2$ $Å^{-1}$, which is higher than that of the peak observed in SiO_2 glass at $Q=1.52$ $Å^{-1}$ (Ref. 31); this implies that the glassy network is no longer formed only by connections of SiO_4 tetrahedra but also PbO_x polyhedra contribute. It is remarkable that a prepeak can be distinguished in the x-ray $S(Q)$ of the 34 mol % PbO glass at $Q \sim 0.4$ $Å^{-1}$ and in the neutron $S(Q)$ of the 65 mol % glass at $Q \sim 1.2$ $Å^{-1}$, respectively. Golubkov *et al.* found small-angle scattering peak in the PbO-SiO_2 glass at PbO concentration <40 mol%,[32] and we observed a similar trend in high-energy x-ray diffraction data for the 30, 34, and 38 mol % PbO glasses as shown in Fig. 2; previous studies did not report such prepeaks in XRD data (e.g., Ref. 12). These characteristic prepeaks in the PbO-SiO_2 glasses imply

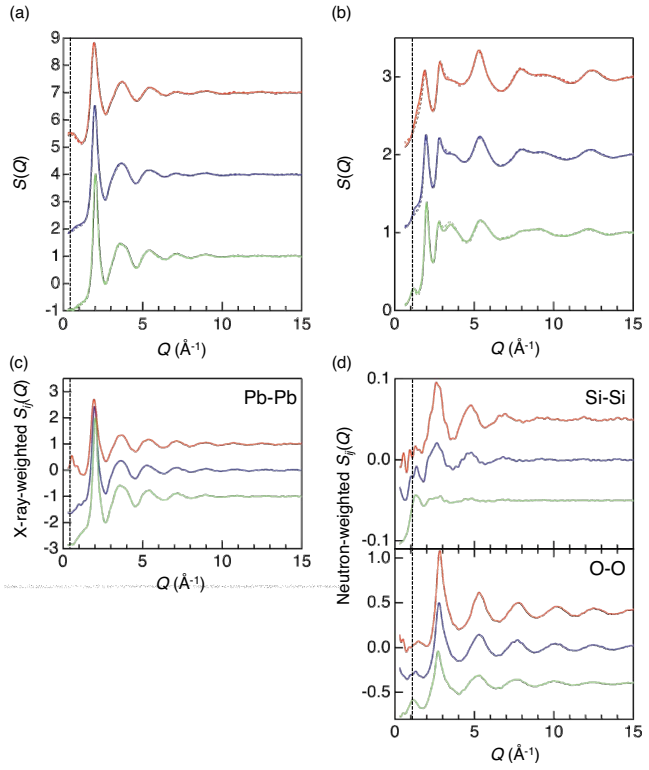

FIG. 1. (Color online) Structure factors for PbO-SiO_2 glasses. (a) X-ray total structure factors $S(Q)$ of PbO-SiO_2 glasses. (b) Neutron total structure factors of PbO-SiO_2 glasses (solid curve, experimental data; dotted curve, RMC model). (c) X-ray and neutron-weighted partial structure factors $S_{ij}(Q)$ of PbO-SiO_2 glasses derived from the RMC model. Red (uppermost curves), 34 mol % PbO; blue (middle curves), 50 mol % PbO; and green (lowermost curves), 65 mol % PbO.

the modification of silicate network formed in SiO_2 glass by addition of PbO.

Figure 3 shows the x-ray (A) and neutron (B) total correlations functions $T(r)$ obtained by Fourier transformation of the $S(Q)$. The typical atomic distances and coordination numbers obtained from diffraction data are summarized in

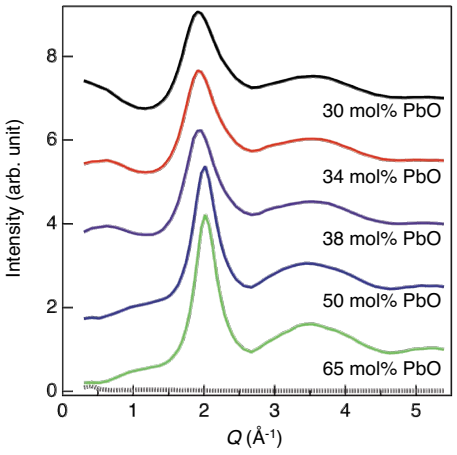

FIG. 2. (Color online) X-ray diffraction patterns for PbO-SiO_2 glasses. Successive curves are displaced upward by 1.5 for clarity. The dotted line represents instrumental background.

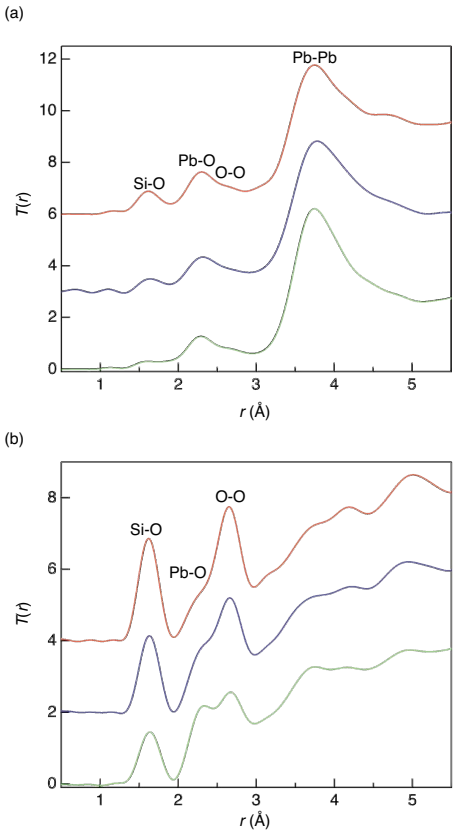

FIG. 3. (Color online) Total correlation functions $T(r)$ for PbO-SiO_2 glasses. (a) X-ray diffraction data. (b) neutron-diffraction data. Red (uppermost curves), 34 mol % PbO; blue (middle curves), 50 mol % PbO; and green (lowermost curves), 65 mol % PbO.

Table I. The Si-O bond length in the PbO-SiO_2 glass is 1.63 Å and the number of oxygen atoms around silicon atoms, i.e., the Si-O coordination number, in all glass compositions appears to be 4 from neutron-diffraction data, demonstrating that SiO_4 tetrahedra are formed in PbO-SiO_2 glasses. Furthermore, it is remarkable that the Pb-O correlation peaks are observed at a short bond length (~2.3 Å) and that the shape of the Pb-O peak is not symmetric. Curve fitting to experimental total correlation functions, using Gaussian functions, yields an average Pb-O coordination number of approximately 4 for all compositions.

To observe the structure of PbO-SiO_2 glasses in detail, we performed structural modeling by employing the RMC simulation technique. The $S(Q)$ derived from the RMC models are plotted in Figs. 1(a) and 1(b) as dotted lines. The agreement between the experimental data and RMC models is excellent. To investigate the origin of the prepeaks ($Q \sim 0.4$–1.2 $Å^{-1}$), we compared the x-ray and neutron-weighted partial structure factors, $S_{ij}(Q)$, derived from the RMC models, with the corresponding experimental $S(Q)$ for all compositions. As can be seen in Figs. 1(c) and 1(d), the weighted Pb-Pb, Si-Si, and O-O $S_{ij}(Q)$ exhibit significant composition-dependent changes. It is remarkable that the Pb-Pb $S_{ij}(Q)$ has a large positive contribution to the prepeak ($Q \sim 0.4$ $Å^{-1}$) in the x-ray $S(Q)$ of the 34 mol % PbO glass whereas the O-O partial has a positive contribution (Q

TABLE I. Parameters of Gaussian functions ($r_{i\text{-}j}$: interatomic distance, FWHM: full width at half maximum, $N_{i\text{-}j}$: coordination number) obtained from the fit of the first-neighbor peaks of Fourier-transformed neutron-diffraction data of PbO-SiO_2 glasses. The distances and FWHM are given in angstrom. Numbers in parentheses give the uncertainty. Pb-O interatomic distances are mean values and the coordination numbers are total values. O-O coordination numbers were fixed to the values calculated from x-ray photoelectron spectroscopy studies (Ref. 33) during the fit.

$(PbO)_x(SiO_2)_{100-x}$ glass sample	$x=0$			$x=34$			$x=50$			$x=65$		
i-j	$r_{i\text{-}j}$	FWHM	$N_{i\text{-}j}$	$r_{i\text{-}j}$	FWHM	$N_{i\text{-}j}$	$r_{i\text{-}j}$	FWHM	$N_{i\text{-}j}$	$r_{i\text{-}j}$	FWHM	$N_{i\text{-}j}$
Si-O	1.61 (1)	0.18 (1)	3.9 (1)	1.63 (1)	0.19 (1)	3.8 (1)	1.63 (1)	0.20 (1)	4.0 (1)	1.63 (1)	0.20 (1)	4.1 (1)
Pb-O (1)				2.31 (2)	0.32 (3)	2.6 (2)	2.32 (2)	0.32 (3)	2.8 (2)	2.28 (2)	0.33 (3)	2.3 (2)
Pb-O (2)				2.70 (2)	0.35 (3)	1.5 (2)	2.77 (2)	0.35 (3)	1.3 (2)	2.68 (2)	0.35 (3)	1.7 (2)
Pb-O				2.46 (2)		4.1 (4)	2.46 (2)		4.1 (4)	2.45 (2)		4.0 (4)
O-O	2.63 (1)	0.23 (1)	5.8 (1)	2.66 (2)	0.24 (2)	4.8	2.65 (2)	0.25 (2)	4.2	2.67 (2)	0.25 (2)	3.7

~ 1.1 Å^{-1}) to the prepeak ($Q \sim 1.2$ Å^{-1}) of the neutron $S(Q)$ of the 65 mol % PbO glass. Moreover, the Si-Si partial has a strong positive contribution ($Q \sim 1.5$ Å^{-1}) to the prepeak of the 65 mol % PbO glass, in which the fraction of silicon is the smallest for all compositions, suggesting that the silicate network is almost broken down at this composition. It is also worth mentioning that the prepeaks ($Q \sim 0.4$–1.2 Å^{-1}) could not be observed in the $S(Q)$ of initial RMC configurations created by HSMC simulations without any experimental data.

From the three-dimensional atomic models by RMC the origin of the prepeaks can be analyzed. In the RMC simulations, the SiO_4 units were constrained because it is well known (and is confirmed by our diffraction data) that SiO_4 tetrahedra form in silicate glasses. The first peak of the Pb-O partial pair distribution functions, $g_{PbO}(r)$ (Fig. 4), is broad and skewed toward the high-r side. The average Pb-O coordination number, calculated from the RMC model up to 3.0 Å, is approximately 4, which is in good agreement with the experimental data suggesting that PbO_x polyhedra occur in all compositions (PbO_4 tetrahedra are in majority, although PbO_3 and PbO_5 are also observed). This result is consistent with the NMR data reported by Fayon *et al.*,[16] demonstrating that lead forms covalent PbO_4 and PbO_3 pyramids over a large compositional range.

Three-dimensional atomic configurations and Q_n distribution of SiO_4 tetrahedra, as obtained from the RMC models, are shown in Figs. 5(a) and 5(b), respectively. The atomic configurations of SiO_4 tetrahedra demonstrate that the network structure formed in SiO_2 glass is significantly broken by the addition of PbO, as the number of bridging oxygen atoms decreases in the 50 mol % PbO glass. It is remarkable that chains consisting of SiO_4 tetrahedra with corner-sharing oxygens, manifested by Q_2, are formed in the 50 mol % glass and there is no ring structure consisting of SiO_4 tetrahedra with corner-sharing oxygens in the 65 mol % PbO glass. Similar behavior—modification of the silicate network—is observed in forsterite (Mg_2SiO_4) glass but the contribution of isolated SiO_4 tetrahedra (75%) in the 65 mol % PbO glass is larger than that in forsterite glass.[34] This breakdown of SiO_4 linkage is well described by the Q_n distributions shown in Fig. 5(b), which are qualitatively consistent with the recent NMR data reported by Takaishi *et al.*[12]

To understand the local structure of PbO_x polyhedra, the O-Pb-O bond-angle distributions have been analyzed [Fig. 6(a)]. Each glass, independent of the composition, exhibits a

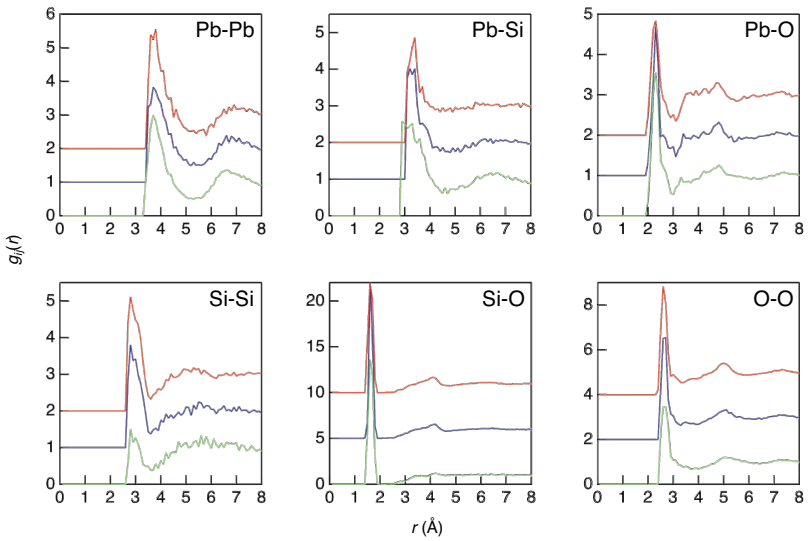

FIG. 4. (Color online) Partial pair distribution functions, $g_{ij}(r)$, of PbO-SiO_2 glasses derived from the RMC models (red (uppermost curves), 34 mol % PbO glass; blue (middle curves), 50 mol % PbO glass; and green (lowermost curves), 65 mol % PbO glass).

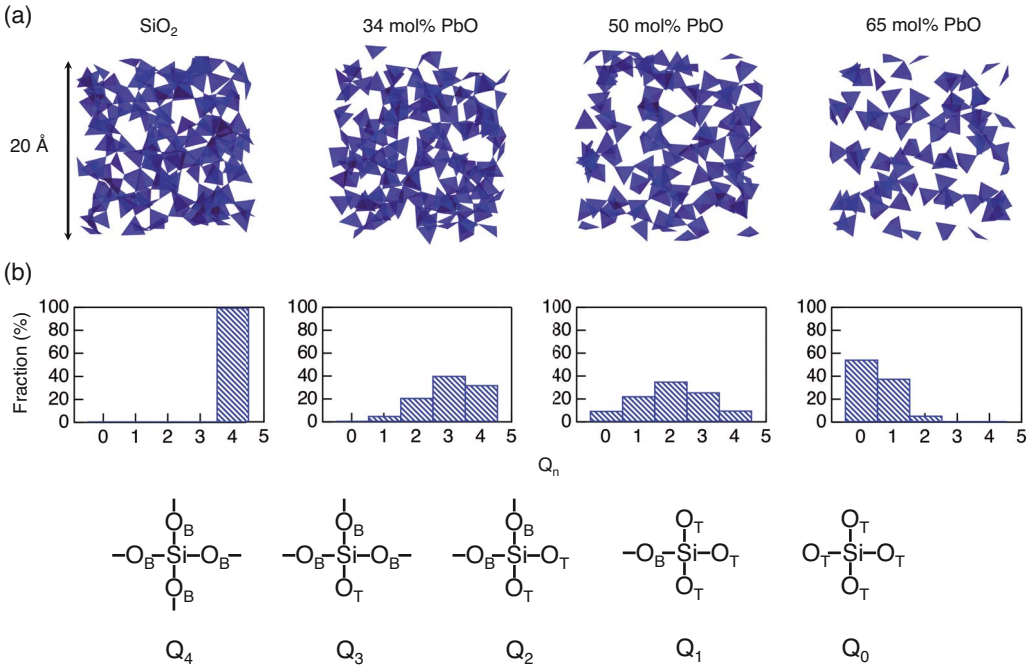

FIG. 5. (Color online) The atomic configuration and Q_n distribution of SiO_4 tetrahedra obtained from the RMC model. (a) The configuration of SiO_4 tetrahedra. (b) Q_n distribution of SiO_4 tetrahedra (O_B, bridging oxygen; O_T, terminal oxygen).

distinct peak at around 60°, suggesting a typical dense random packing which occurs in most disordered systems.[35] The other, broader, maximum is centered at around 110°, indicating tetrahedral local ordering. The feature of the O-Pb-O bond-angle distribution may be smeared out, so that it is probably sharper in the real material, as RMC is known to produce the most disordered structure[36] which is consistent with a given set of diffraction data and geometrical constraints. Figure 6(b) shows a typical atomic configuration of PbO_4 polyhedra in the 34 mol % PbO glass. It is noted that the position of lead is off-centered within the polyhedron, and that the shape of PbO_4 polyhedra in PbO-SiO_2 glasses is not a regular tetrahedron but rather similar to a square pyramid found in the PbO crystal.[37]

Figure 6(c) shows the results of connectivity analysis for SiO_4-SiO_4 and for PbO_x-PbO_x polyhedra. These results demonstrate that SiO_4 tetrahedra are network formers in the 34 mol % PbO glass, and that the role of network former is obviously replaced by PbO_x polyhedra in the 50 mol % PbO glass. A large fraction of PbO_x polyhedra do not participate in network formation (non-network PbO_x unit), and they are manifested by isolated short chains or complex units in the 34 mol % PbO glass (yellow colored polyhedra in Fig. 7). This is in sharp contrast with the behavior of SiO_4 tetrahedra in the 65 mol % PbO glass, where strong Si-O covalent bonds form mainly isolated SiO_4 tetrahedra and Si_2O_7 dimers (i.e., not chains or larger units, see Fig. 5) while the network structure is largely composed of connected PbO_x polyhedra shown as a red colored part in Fig. 7). Such behavior is qualitatively consistent with the model proposed by Mizuno *et al.*[38]

At this point, we are able to discuss the origin of the two characteristic peaks observed at $Q \sim 0.4$ Å^{-1} in the x-ray $S(Q)$ of the 34 mol % PbO glass and at $Q=1.2$ Å^{-1} in the neutron $S(Q)$ of the 65 mol % glass. In the 34 mol % PbO glass, the atomic configuration reveals that the distribution of PbO_x polyhedra is not entirely uniform (Fig. 7). This feature is well represented by the inhomogeneous distribution of lead in the 34 mol % PbO glass shown in Fig. 6(c) whereas neither the 50 mol % nor the 65 mol % PbO glass exhibits such an inhomogeneous lead distribution. Hence, this inhomogeneous distribution of Pb, induced by the separation of network and non-network PbO_x units, is the origin of the characteristic peak at $Q=0.4$ Å^{-1} in the x-ray $S(Q)$ of the 34 mol % PbO glass. Indeed, Pb forms large "cages" (i.e., volumes where lead atoms are absent) with the Pb-Pb bond connection having ~5.3 Å distance (within the first Pb-Pb coordination shell, see Fig. 4). As it is indicated by an arrow in Fig. 6(c), the typical size of the large cage is about 15 Å, corresponding to $Q \sim 0.4$ Å^{-1}, and this matches well with the position of the prepeak in the x-ray data of the 34 mol % PbO glass. Such an inhomogeneous distribution of PbO_x polyhedra was not present in the initial configuration of RMC modeling, and it was therefore produced as a consequence of introducing the diffraction data. Accordingly, the final RMC model reflects the low-Q feature of the $S(Q)$. Furthermore, no PbO-SiO_2 crystal with diffraction peaks at around such a low-Q (~0.4 Å^{-1}) has been reported. Hence this structural inhomogeneity beyond the atomic scale is a unique structural feature of the 34 mol % PbO glass. In the case of the 65 mol % PbO glass, inhomogeneous distribution of SiO_4 units, i.e., the formation of isolated SiO_4 tetrahedra and Si_2O_7 dimers (54% and 17% of SiO_4 tetrahedra form SiO_4 and Si_2O_7, respectively) give rise to a peak of the neutron $S(Q)$ at a position of a lower Q value than $Q=1.52$ Å^{-1} (signature of silicate network).

The atomic number densities of PbO-SiO_2 glasses are almost constant over a wide composition range (SiO_2 glass:

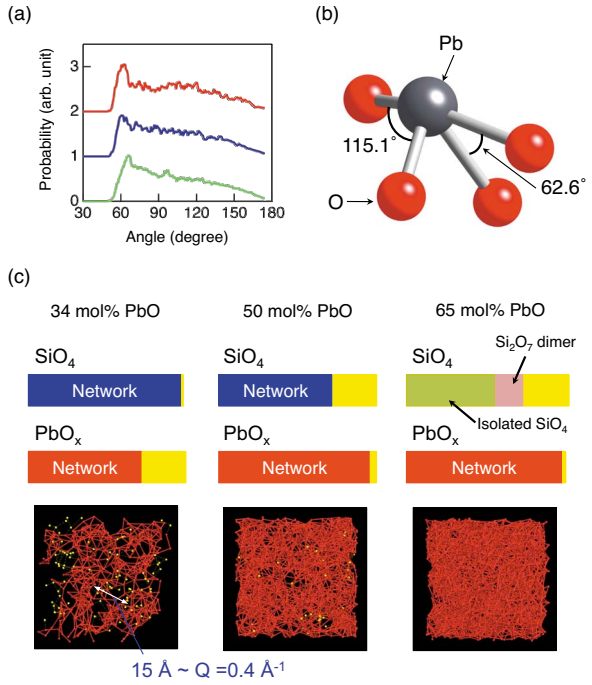

FIG. 6. (Color online) The atomic configuration of PbO_x polyhedra and the network connectivity of SiO_4 tetrahedra and PbO_x polyhedra. (a) O-Pb-O and bond-angle distribution of PbO-SiO_2 glasses. Red [uppermost curve in part (a)], 34 mol % PbO glass; blue [middle curve in part (a)], 50 mol % PbO glass; and green [lowermost curve in part (a)], 65 mol % PbO. (b) Typical connectivity of PbO_4 tetrahedron taken from a RMC snapshot of the 34 mol % PbO glass (magenta, lead; red, oxygen). (c) Bar chart of network connectivities and the distribution of lead in PbO-SiO_2 glass (the red colored bonds mean correlation between Pb atoms in the network unit). In the 34 mol % PbO glass, 99% of SiO_4 tetrahedra form network, and 72% and 28% of PbO_x polyhedra form network and non-network units, respectively. In the 50 mol % PbO glass, 96% of PbO_x polyhedra form network, and 74% of SiO_4 tetrahedra form network, respectively. In the 64 mol % PbO glass, 99% of PbO_x polyhedra form network, and 54% and 17% of SiO_4 tetrahedra form SiO_4 and Si_2O_7, respectively. SiO_4 tetrahedra also form isolated chains or more complex units with ~60 Si and O atoms in the 50 and 64 mol % PbO glasses.

0.066 $Å^{-3}$, 34 mol % PbO glass: 0.065 $Å^{-3}$, 50 mol % PbO glass: 0.063 $Å^{-3}$, 65 mol % PbO glass: 0.059 $Å^{-3}$) and are very low compared with those of typical binary ox-

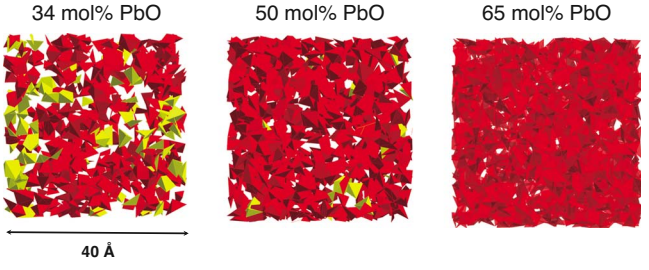

FIG. 7. (Color online) The configuration of PbO_x polyhedra obtained from a RMC snapshot. The red colored part (dark gray) and yellow colored parts (light gray) represent network unit and non-network units, respectively.

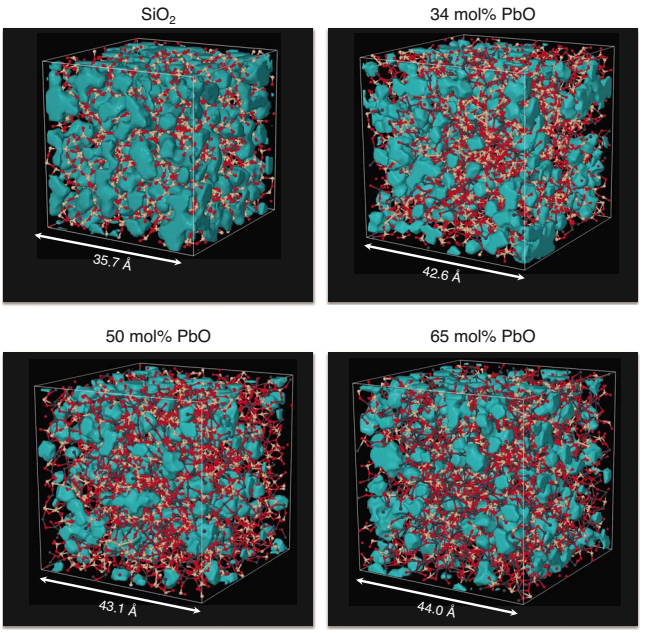

FIG. 8. (Color online) The atomic configuration and voids of SiO_2 glass (3000 atoms) and PbO-SiO_2 glasses (5000 atoms). Color key: light gray, silicon; red (dark gray), oxygen; gray, lead, and cyan; voids (gray tone).

ide glasses (43 mol % Na_2O-57 mol % SiO_2 glass: 0.076 $Å^{-3}$, 43 mol % CaO-57 mol % SiO_2 glass: 0.074 $Å^{-3}$).[39] This feature is clearly visible in the atomic configurations shown in Fig. 8, where the voids (free volume) have been highlighted. The total volume occupied by the voids is 31.9% (SiO_2 glass), 15.4% (34 mol % PbO glass), 11.3% (50 mol % PbO glass), and 12.6% (65 mol % PbO glass). The most surprising feature is that more than 10% of the volume assigned to voids can be observed over a wide composition range, compared with almost no voids in the RMC models of 43 mol % Na_2O-57 mol % SiO_2 and 43 mol % CaO-57 mol % SiO_2 silicate glasses.[39] Large amounts of free volume (voids) cannot be found in conventional binary silicate glasses, such as Na_2O-SiO_2 and CaO-SiO_2 (network former—network modifier), but only in network-former glasses, such as SiO_2 glass, and in its mixtures with another network former such as GeO_2. Hence, it is necessary to classify PbO-SiO_2 glass as a "binary network-former glass." Consequently, PbO-SiO_2 glass can be considered as a network-former glass even to the extent of binary silicates because the large amount of free volume can accommodate additional cations from a network modifier.

V. CONCLUSION

PbO-SiO_2 glasses have been widely studied over 20 years and many small-scale and oversimplified structural models, regardless of being consistent with diffraction data, have been proposed. In this study, we employed various diffraction experiments and performed structural modeling in order to understand the detailed atomic structure on the basis of experimental data. A combination of x-ray and neutron-diffraction data, aided by reverse Monte Carlo structural

modeling, has been proven to be able of revealing the structure of PbO-SiO_2 glasses over a wide composition range. Based on the large particle configurations that are fully consistent with measured data the following conclusions may be drawn:

(1) the structure of PbO-SiO_2 glass can be categorized as a binary network-former glass with a large amount of free volume.

(2) The formation of the network is governed by the interplay of SiO_4 tetrahedra and PbO_x polyhedra as network formers while the other non-network units are distributed inhomogeneously. This behavior is out of the concept of Zachariasen's CRN theory (modified by Warren) which describes the structure of a "network-former glass" and "network former—modifier glass." CRN does not consider long-range concentration fluctuations since it evolved from only the structural information on short-range order in related crystals and from the knowledge that a network can be formed by these short-range-ordered units in oxide glasses.

Thus a structural study such as described here, by making large-scale structure models, is indispensable for understanding the rather complex structure of glass and its relationship to physicochemical properties of glasses.

ACKNOWLEDGMENTS

We thank Jan Swenson for providing us with the atomic configuration of 43 mol % Na_2O-57 mol % SiO_2 and 43 mol % CaO-57 mol % SiO_2 glasses. Discussions with D. L. Price, Marie-Louise Saboungi, and A. Fujiwara are greatly appreciated. The synchrotron radiation experiment was carried out with the approval of the Japan Synchrotron Radiation Research Institute (JASRI) (Proposal No. 2002B0702-ND1-np). S.K., T.U., and J.A. are supported by the Japan Science and Technology Agency and the Academy of Finland via the Strategic Japanese-Finland Cooperative Program on "Functional Materials." L.P. is grateful to the Japanese Society for the Promotion of Science.

[1] W. H. Zachariasen, J. Am. Chem. Soc. **54**, 3841 (1932).
[2] B. E. Warren, J. Am. Ceram. Soc. **24**, 256 (1941).
[3] S. C. Moss and D. L. Price, in *Physics of Disordered Materials*, edited by D. Adler, H. Fritzsche, and S. R. Ovshinsky (Plenum, New York, 1985), p. 77.
[4] S. R. Elliott, Nature (London) **354**, 445 (1991).
[5] P. S. Salmon, R. A. Martin, P. E. Mason, and G. J. Cuello, Nature (London) **435**, 75 (2005).
[6] C. C. Wang, Phys. Rev. B **2**, 2045 (1970).
[7] J. L. Wiza, Nucl. Instrum. Methods **162**, 587 (1979).
[8] H. Morikawa, Y. Takagi, and H. Ohno, J. Non-Cryst. Solids **53**, 173 (1982).
[9] M. Imaoka, H. Hasegawa, and I. Yasui, J. Non-Cryst. Solids **85**, 393 (1986).
[10] K. Suzuya, S. Kohara, and H. Ohno, Jpn. J. Appl. Phys., Suppl. **38**, 144 (1999).
[11] U. Hoppe, R. Kranold, A. Ghosh, C. Landron, J. Neuefeind, and P. Jóvári, J. Non-Cryst. Solids **328**, 146 (2003).
[12] T. Takaishi, M. Takahashi, J. Jin, T. Uchino, and T. Yoko, J. Am. Ceram. Soc. **88**, 1591 (2005).
[13] C. A. Worrell and T. Henshall, J. Non-Cryst. Solids **29**, 283 (1978).
[14] A. M. Zahra and C. Y. Zahra, J. Non-Cryst. Solids **155**, 45 (1993).
[15] P. W. Wang and L. Zhang, J. Non-Cryst. Solids **194**, 129 (1996).
[16] F. Fayon, C. Bessada, D. Massiot, I. Farnan, and J. P. Coutures, J. Non-Cryst. Solids **232-234**, 403 (1998); F. Fayon, C. Landron, K. Sakurai, C. Bessada, and D. Massiot, *ibid.* **243**, 39 (1999).
[17] K. N. Dalby and P. L. King, Am. Mineral. **91**, 1783 (2006).
[18] J. Rybicki, A. Rybicka, A. Witkowska, G. Bergmański, A. Di Cicco, M. Minicucci, and G. Mancini, J. Phys.: Condens. Matter **13**, 9781 (2001).
[19] K. H. Sun, J. Am. Ceram. Soc. **30**, 277 (1947).
[20] M. Isshiki, Y. Ohishi, S. Goto, K. Takeshita, and T. Ishikawa, Nucl. Instrum. Methods Phys. Res. A **467-468**, 663 (2001).
[21] S. Kohara, M. Itou, K. Suzuya, Y. Inamura, Y. Sakurai, Y. Ohishi, and M. Takata, J. Phys.: Condens. Matter **19**, 506101 (2007).
[22] S. Sasaki, KEK Report No. 90-16, 1991 (unpublished).
[23] D. T. Cromer, J. Chem. Phys. **50**, 4857 (1969).
[24] D. Waasmaier and A. Kirfel, Acta Crystallogr., Sect. A: Found. Crystallogr. **51**, 416 (1995).
[25] A. J. G. Ellison, R. K. Crawford, D. G. Montague, K. J. Volin, and D. L. Price, J. Neutron Res. **1**, 61 (1993).
[26] A. C. Hannon, W. S. Howells, and A. K. Soper, *Neutron Scattering Data Analysis*, IOP Conf. Proc. No. 107 (Institute of Physics and Physical Society, London, 1990), p. 193.
[27] T. E. Faber and J. M. Ziman, Philos. Mag. **11**, 153 (1965).
[28] E. A. Lorch, J. Phys. C **2**, 229 (1969).
[29] R. L. McGreevy and L. Pusztai, Mol. Simul. **1**, 359 (1988).
[30] J. Akola and R. O. Jones, Phys. Rev. B **76**, 235201 (2007).
[31] S. Kohara and K. Suzuya, J. Phys.: Condens. Matter **17**, S77 (2005).
[32] V. V. Golubkov V. N. Bogdanov, A. Ya Pakhnin, V. A. Solovyev, E. V. Zhivaeva, V. O. Kabanov, O. V. Yanush, S. V. Nemilov, A. Kisliuk, M. Soltwisch, and D. Quitmann, J. Chem. Phys. **110**, 4897 (1999).
[33] B. M. J. Smets and T. P. A. Lommen, J. Non-Cryst. Solids **48**, 423 (1982).
[34] S. Kohara, K. Suzuya, K. Takeuchi, C.-K. Loong, M. Grimsditch, J. K. R. Weber, J. A. Tangeman, and T. S. Key, Science **303**, 1649 (2004).
[35] M. A. Howe, R. L. McGreevy, L. Pusztai, and I. Borzsák, Phys. Chem. Liq. **25**, 205 (1993).
[36] M. T. Dove, M. G. Tucker, and D. A. Keen, Eur. J. Mineral. **14**, 331 (2002).
[37] J. Leciejewicz, Acta Crystallogr. **14**, 1304 (1961).
[38] M. Mizuno, M. Takahashi, T. Takaishi, and T. Yoko, J. Am. Ceram. Soc. **88**, 2908 (2005).
[39] C. Karlsson, E. Zanghellini, J. Swenson, B. Roling, D. T. Bowron, and L. Börjesson, Phys. Rev. B **72**, 064206 (2005).